Available online at www.sciencedirect.com

ScienceDirect

Energy Procedia 156 (2019) 417–424

Energy Procedia

www.elsevier.com/locate/procedia

2018 5th International Conference on Power and Energy Systems Engineering, CPESE 2018, 19–21 September 2018, Nagoya, Japan

Microgrids Impact on Power System Frequency Response

Hêmin Golpîra[a], and Hassan Bevrani[a,*]

[a] *Smart/Micro Grids Research Center, University of Kurdistan, Sanandaj, 66177-15175, Iran*

Abstract

Microgrid (MG), as a cluster of Distributed Generations (DGs) and local loads, may be characterized with zero or small inertia constant. Reduction of system rotational inertia, in response to increasing MGs penetration level, renders frequency dynamics faster. This paper presents an attempt to propose a new analytical approach to mathematically assess the impact of MGs penetration level on power system frequency stability. In this way, an experimental-based model is employed to make the simulation results realistic. The method interprets the frequency dynamic behavior of the penetrated system based on the conventional system in terms of frequency nadir, steady state deviation and a 15-second rolling window.

Keywords: Frequency stability, Rotational inertia, Microgrids, Frequency nadir, 15-Second rolling window;

1. Introduction

Next generation grids face new technical challenges arising from the increasing penetration of Distributed Generations (DGs), visualized through the Microgrid (MG) concept [1]. While low penetration of MGs has negligible influence on host grid stability, the ability of the system to accommodate high penetration of MGs is in concern [2, 3]. This means that high-penetration of MGs may create stability issues that must be addressed [4]. This paper focuses on frequency stability problem in penetrated power grids.

* Corresponding author. Tel/Fax: +98-87-33660073.
E-mail address: bevrani@uok.ac.ir

1876-6102 © 2019 The Authors. Published by Elsevier Ltd.

10.1016/j.egypro.2018.11.097

Abnormal frequency deviation may significantly affect power system behavior by triggering the protection devices, which, in turn, may initiate frequency instability [5, 6]. Indeed, reduced inertia constant in the system with high MGs penetration jeopardizes system dynamics and stability [3, 7]. Therefore, reduction of system inertia, which renders frequency dynamics faster, introduces one of the impediments to realize high MGs penetration level.

General overview regarding the effects of low inertia on power system frequency stability has been provided in [7]. A trial and error-based methodology is proposed in [8, 9] to determine the maximum permissible penetration level of wind farms. Transit stability assessment of penetrated power system is done in [10, 11]. Ref. [12] deals with scenario-based approach focusing on system inertia and primary reserve values. To study changing trends in frequency behavior of a penetrated power system, a simplified frequency model accompanied with simulation of wind penetration scenarios are employed in [13]. Another scenario-based approach, applied to a part of Australian grid, is discussed in [14]. A new automatic generation control structure, which tackles intermittency drawbacks stemming from high penetration of MGs into problem formulation, is proposed in [15].

While previous studies deal with the effects of MGs penetration level on host grid stability, most of them have varied the penetration level on low dimension systems based on trial and error. Increasing penetrated system dimensions significantly enlarges feasible space of scenarios to be assessed in trial and error procedure. On the other hand, the so far researches consider constant parameters for the MGs in the trial and error procedure. Indeed, the intermittent inherent of MGs provides time-variant parameters, such as rotational inertia [7], which in turn may affect penetrated system dynamics in response to a given fault. Lack of analytical approaches for assessing of MGs penetration level on host grid frequency stability makes the so far researches far from realistic. An attempt is made in this paper to propose a mathematical-based approach to analytically investigate the effect of rotational inertia reduction, i.e. MGs penetration level, on frequency dynamics. Here, frequency dynamics such as frequency nadir, 15-second rolling window and steady-state deviation are employed to establish a mathematical-based case independent approach.

Nomenclature

MG	microgrid
DG	distributed generator
ESS	energy storage system
WT	wind turbine
PV	photovoltaic
SS	static switch
RMSE	root mean square error
UCTE	Union for the Coordination of the Transmission of Electricity
COI	center of inertia
NERC	North American Electric Reliability Corporation

2. Proposed Analytical Approach

Concerning the frequency response dynamics, it is assumed that H describes the aggregated inertia of different generators and load nodes.

1.1. Definitions

Derivation of an analytical approach to investigate the impact of MGs penetration level on the host grid frequency stability begins through defining of two systems, as follows:

a) *Base system*: It referred to as the original system without any MGs. Base system characterized by its known inertia, damping constants and frequency dynamics.
b) *Penetrated system*: The second system, referred to as the reduced inertia system characterized with unknown frequency dynamics, is the base system after penetration of MGs.

Frequency dynamics may be assessed in respect to several criteria such as, frequency nadir, steady state deviation and a 15-second rolling window [5]. These criteria are employed in this paper to establish a systematic approach to deal with the impact of inertia-less sources on the host grid frequency stability.

1.2. MG Structure

In order to visualize integrated grid, the available MG in the Smart/Micro Grids Research Center (SMGRC) at the University of Kurdistan (UOK) is employed, that here it is called UOK-MG. It includes Energy Storage Systems (ESSs) and several micro sources (PV, WT, and diesel generator) as shown in Figure 1 (Fig. 1a). A view of SMGRC data acquisition and monitoring system is also shown in Fig. 1b. Experimental and simulation results of the UOK-MG in both grid-connected and island mode are compared in this section. Afterwards, the results of UOK-MG in grid connected mode is extended to realize the high penetrated grid, as introduced in [16].

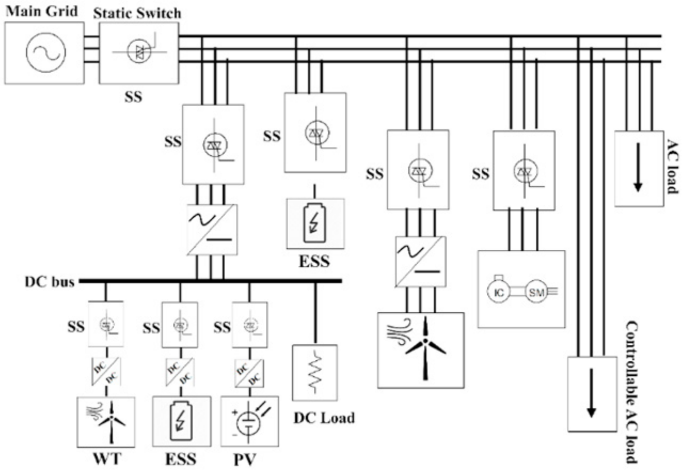

(a)

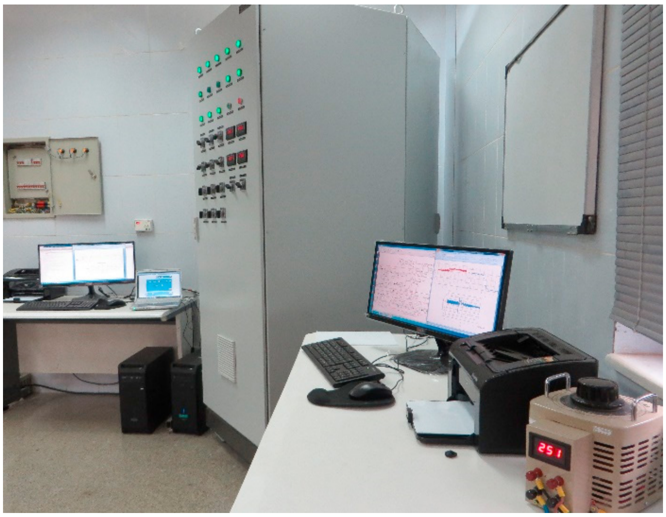

(b)

Fig. 1. UOK experimental system, a) Three-phase representation of UOK-MG, and b) Data acquisition and monitoring unit

In island mode, the diesel generator is modeled by an internal combustion engine driven and a field wound synchronous generator. On the other hand, the inverter-based sources employ frequency and voltage droop characteristics to control the output active and reactive powers [4, 16, 17]. The used models are realistic and practically validated by comparison with actual results. For instance, Figure 2 compares the ESS simulation results, obtained for a step increase in load at 4th second of the simulation, with those of experimental dynamics.

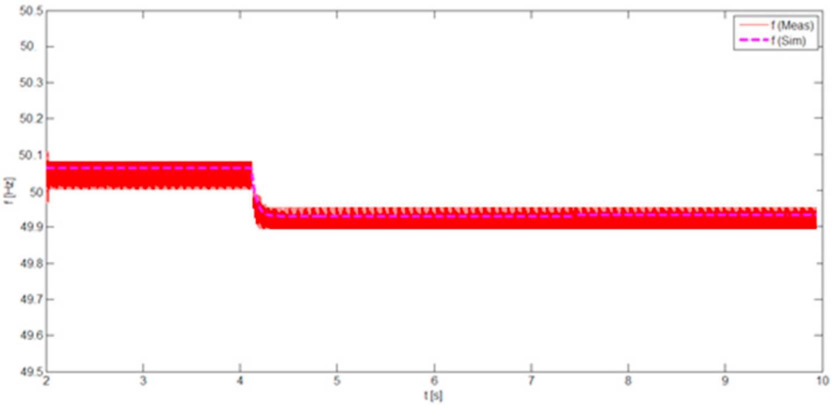

Fig. 2. Frequency dynamics of ESS in response to switching on of R_2 in 4th second of the simulation

In the grid connected mode, MG dynamics, from upward point of view, may be represented through a set of inertia constant and load damping parameters. Details of such representation can be found in [18, 19]. Indeed, the experimental results reveal that there is a direct relationship, with Root Mean Square Error (RMSE) equal to 0.2165, between the MG inertia and the ratio of diesel generator to the MG capacity.

1.3. Frequency Nadir

Minimum instantaneous frequency, known as frequency nadir, is defined as the first index of interest to deal with the penetrated system. The frequency nadir is defined to be 49.2 [Hz] based on the *Union for the Coordination of the Transmission of Electricity (UCTE)* standards [20].

Any instantaneous change in system frequency, would be represented by the swing equation as [5]:

$$\frac{2H_i}{\omega_0}\frac{d^2\theta}{dt^2} = \omega_i(\mathrm{T}_{mech} - \mathrm{T}_{elec}) \xrightarrow{\theta=\omega_i t - \omega_0 t + \theta_0} 2H_i \frac{d(\Delta f_i)}{dt} = 2\pi f_i(\mathrm{T}_{mech} - \mathrm{T}_{elec}) \tag{1}$$

Using (1), the frequency responses of the base and the penetrated systems, for a given fault, are as:

$$2H_1\frac{d(\Delta f_1)}{dt} = 2\pi f_1(\mathrm{T}_{mech} - \mathrm{T}_{elec}) \tag{2}$$

and

$$2H_2\frac{d(\Delta f_2)}{dt} = 2\pi f_2(\mathrm{T}_{mech} - \mathrm{T}_{elec}) \tag{3}$$

Dividing (3) by (2) gives:

$$\frac{H2}{H1}.\frac{d(\Delta f_2)}{d(\Delta f_1)} = \frac{f_2}{f_1} \xrightarrow{\times\frac{\Delta f_1}{\Delta f_1}} \frac{H2}{H1}.\frac{d(\Delta f_2)}{d(\Delta f_1)}.\Delta f_1 = \frac{\Delta f_1}{f_1} f_2 \tag{4}$$

The term $\frac{d(\Delta f_2)}{d(\Delta f_1)}$ in (4) describes the sensitivity of frequency deviation for the penetrated system to frequency deviation of the base system. Multiplying by the base system frequency change for a given fault, i.e. Δf_1, it reflects the frequency change of the penetrated system. This means that, (4) could represent the penetrated system frequency dynamics based on the base system response for a given fault.

Here, it should be noted that (4) is derived for the aggregated inertia of all areas. In order to assess frequency dynamics in a typical area in an interconnected power system, the interactions between areas as well as load dynamics (D) should be accounted in the problem formulation. For this purpose, (1) can be rewritten as [7]:

$$\dot{f}_i = \frac{1}{2\pi M_i}[\Delta P_i - 2\pi D_i f_i - \sum_j P_{tie,ij}]\,, i, j = 1,...,n\,, i \neq j \tag{5}$$

where, $P_{tie,ij}$, n, M, D are the tie-line power between areas i and j, number of areas, inertia constant and load damping, respectively. One could re-write the deviation of $P_{tie,ij}$ from the pre-fault steady state value, using Taylor expansion, as follows

$$\begin{aligned} P_{tie,0} + \Delta P_{tie} = P_{tie,0} + 2\pi \mathrm{P}_{\max}(f_i - f_j)Cos(\delta_{i0} - \delta_{j0}).(\delta_i - \delta_j - \delta_{i0} - \delta_{j0}) + [2\pi \mathrm{P}_{\max}(\dot{f}_i - \dot{f}_j)Cos(\delta_{i0} - \delta_{j0}) \\ -2\pi \mathrm{P}_{\max}(f_i - f_j)\sin(\delta_{i0} - \delta_{j0})].(\delta_i - \delta_j - \delta_{i0} - \delta_{j0})^2 \end{aligned} \tag{6}$$

Then, $(\dot{f}_i - \dot{f}_j)$ in (6) could be replaced by the aggregated model of non-coherent generators as represented by (7).

$$\dot{f}_i - \dot{f}_j = \frac{1}{2\pi}\frac{H_i + H_j}{2H_i H_j}[\frac{H_i}{2H_i H_j}(\mathrm{P}_{\mathrm{m}i} - \mathrm{P}_{\mathrm{e}i}) - \frac{H_j}{2H_i H_j}(\mathrm{P}_{\mathrm{m}j} - \mathrm{P}_{\mathrm{e}j})] \tag{7}$$

Representation of the *n-area* penetrated system dynamics by (5)-(7), gives $n-1$ independent equations, with n unknown nadirs, as given by (8):

$$F_i(F_1^{nadir}, F_2^{nadir}, ..., F_j^{nadir}) = 0;\ j = 1,2,...,n;\ i = 1,2,...,n-1 \tag{8}$$

In order to solve set (8), the $n-th$ equation would be formulated based on the frequency response of overall system center of inertia (COI). For this purpose, the COI for the overall system in response to disturbance/fault would be calculated by (5). The result then would be tied to (9) to calculate the $n-th$ equation.

$$\Delta f_{COI} = \frac{\sum_i H_i \Delta f_i}{\sum H_i} \tag{9}$$

1.4. Frequency Change Detection

Based on the introduced criterion by NERC resource subcommittee, a frequency event is detected if during a 15-second rolling time window, the frequency deviation exceeds the specific frequency threshold [21]. The frequency response in Laplace domain for area i in an interconnected power system would be described by [22]:

$$(\Delta P_{mi} - \Delta P_{Li} - \Delta P_{tie,ij}).\frac{1}{M_i s + D_i} = \Delta f_i \xrightarrow[\Delta P_{mi} = -\frac{1}{R_i}\Delta f_i]{\Delta P_{tie} = \frac{2\pi}{s}T_{ij}(\Delta f_i - \Delta f_j)} \Delta f_i = -\frac{\Delta P_L - \frac{2\pi T_{ij}}{s}\Delta f_j}{M_i s + D_i + \frac{1}{R_i} + \frac{2\pi T_{ij}}{s}} \tag{10}$$

where, R is the droop characteristic.

The rolling manner of this criterion is visualized through explanation of the frequency dynamics as a function of time, i.e. t. Generally, for the load disturbance analysis, ΔP_{Li} is usually considered in the form of a step function, i.e. $\Delta P_{Li}(s) = \frac{\Delta P_{Li}}{s}$. Therefore, one could rewrite (10) as follows:

$$\Delta f_i = -\frac{\frac{\Delta P_L}{s} - \frac{2\pi T_{ij}}{s}\Delta f_j}{M_i s + D_i + \frac{1}{R_i} + \frac{2\pi T_{ij}}{s}} = \frac{\Delta P_L - 2\pi T_{ij}\Delta f_j}{M_i s^2 + (D_i + \frac{1}{R_i})s + 2\pi T_{ij}} \tag{11}$$

Inverse Laplace transformation of (11) gives

$$\Delta f_i(t) = -(\frac{\Delta P_L - 2\pi T_{ij}\Delta f_j}{M_i})(\frac{1}{b-a})(e^{-at} - e^{-bt}), \tag{12}$$

where, a, b are the poles of (11). In order to develop an index in compliance with this criterion, the frequency at the end of 15-second rolling window should be employed. For this purpose, at the end of the 15-second rolling window, frequency deviation is represented by:

$$\Delta f_i = -(\frac{\Delta P_L - 2\pi T_{ij}\Delta f_j}{M_i})(\frac{1}{b-a})(e^{-a(t+15)} - e^{-b(t+15)}) \tag{13}$$

Following dividing (13) by (12) and using (4), the frequency deviation during 15-second rolling window for the penetrated system can be determined. In this way, the term $D_i + \frac{1}{R_i}$ in (13) may be calculated through utilization of steady state frequency deviation. According to (4), one can give:

$$\frac{\Delta f_{1i}}{\Delta f_{2i}} = \frac{D_{2i} + \frac{1}{R_{2i}}}{D_{1i} + \frac{1}{R_{1i}}} \tag{14}$$

Eq. (14) represents the penetrated system frequency dynamics based on the base system response.

3. Simulation and Numerical Results

The capability of the proposed indices is investigated on the IEEE 16-machine test system, i.e. *New York/New England 68 Bus system* [23]. Assessment of the proposed analysis approach in compliance with the frequency nadir is done through tripping generator number 13, a large and heavy loaded generating unit located in area 2, without any fault. Calculation of frequency nadir related to each area is done through (8). In this way, one could write:

$$0.11\Delta f_1\Delta f_3 + 0.33\Delta f_1\Delta f_4 - 0.02\Delta f_3\Delta f_4 - 0.15\Delta f_3\Delta f_5 = 0.092 \tag{15}$$

$$0.01\Delta f_2\Delta f_3 + 0.43\Delta f_2\Delta f_4 - 0.17\Delta f_3\Delta f_5 - 0.27\Delta f_4\Delta f_5 = 0.312 \quad (16)$$

$$0.67\Delta f_3\Delta f_1 + 0.03\Delta f_3\Delta f_2 - 0.07\Delta f_1\Delta f_4 - 0.83\Delta f_1\Delta f_5 = 0.762 \quad (17)$$

$$0.67\Delta f_2\Delta f_4 + 0.03\Delta f_1\Delta f_4 - 0.07\Delta f_1\Delta f_5 - 0.83\Delta f_1\Delta f_3 = 0.111 \quad (18)$$

As stated, the n^{th} equation should be formulated based on the overall system COI. Using (9), one could write:

$$\Delta f_{COI} = \frac{\Delta P_L \times \Delta P_L}{4HR} = \frac{\sum_i H_i \Delta f_i}{\sum H_i} = 0.32\Delta f_1 + 0.42\Delta f_2 + 0.54\Delta f_3 + 0.76\Delta f_4 + 0.52\Delta f_5 = 1.23 \quad (19)$$

Solving the system of equations (15)-(19) gives rise to the specification of frequency nadir in each area. Table I reports error of frequency nadir, and frequency deviation in 15-second rolling window for the proposed method and simulation results. Results demonstrate the high efficiency of the proposed method.

Table 1. Comparison of simulation and analysis results

Disturbance	Nadir error [%]	15-sec error [%]
G_{13} outage	1.3	0.11

4. Conclusion

A mathematical-based approach has been proposed to deal with the frequency response of a penetrated power grid. The proposed method relies on the basic power system equations which, in turn, make the formulations completely independent of the test case. Development of such case-independent method appropriately overcomes the difficulties associated with the system dimensions. Simulation results reveal that the proposed method could calculate the penetrated system frequency dynamics with error less than 2%. Several aspects of the analysis of MGs on system dynamic behavior deserve further investigation including the effect virtual inertia on frequency stability and the effect of MGs penetration level on the rotor and voltage stabilities.

Acknowledgements

This research is partially supported by the Smart/Micro Grids Research Center at the University of Kurdistan (Iran) and the Alexander von Humboldt Foundation (Germany).

References

[1] R.H. Lasseter, Smart Distribution: Coupled Microgrids, Proceedings of the IEEE, 99 (2011) 1074-1082.
[2] N. Hatziargyriou, H. Asano, R. Iravani, C. Marnay, Microgrids: an overview of ongoing research, development, and demonstration projects, IEEE Power Energy Magazine, (2007) 78-94.
[3] H. Golpîra, H. Seifi, A.R. Messina, M.R. Haghifam, Maximum Penetration Level of Micro-Grids in Large-Scale Power Systems: Frequency Stability Viewpoint, IEEE Transactions on Power Systems, 31 (2016) 5163-5171.
[4] H. Bevrani, B. François, T. Ise, Microgrid Dynamics and Control, John Wiley & Sons, 2017.
[5] H. Bevrani, Robust power system frequency control, Springer, 2008.
[6] H. Golpîra, A.R. Messina, A Center-of-Gravity-Based Approach to Estimate Slow Power and Frequency Variations, IEEE Transactions on Power Systems, 33 (2018) 1026-1035.
[7] A. Ulbig, T.S. Borsche, G. Andersson, Impact of Low Rotational Inertia on Power System Stability and Operation, arXiv preprint arXiv:1312.6435, (2013).
[8] E. Vittal, A. Keane, M. O'Malley, Varying penetration ratios of wind turbine technologies for voltage and frequency stability, in: Power and Energy Society General Meeting-Conversion and Delivery of Electrical Energy in the 21st Century, 2008 IEEE, IEEE, 2008, pp. 1-6.
[9] G. Lalor, A. Mullane, M. O'Malley, Frequency control and wind turbine technologies, Power Systems, IEEE Transactions on, 20 (2005) 1905-1913.
[10] K. Folly, S. Sheetekela, Impact of fixed and variable speed wind generators on the transient stability of a power system network, in: Power Systems Conference and Exposition, 2009. PSCE'09. IEEE/PES, IEEE, 2009, pp. 1-7.
[11] A. Mitra, D. Chatterjee, A sensitivity based approach to assess the impacts of integration of variable speed wind farms on the transient stability of power systems, Renewable Energy, 60 (2013) 662-671.

[12] F. Fernandez-Bernal, I. Egido, E. Lobato, Maximum wind power generation in a power system imposed by system inertia and primary reserve requirements, Wind Energy, 18 (2014) 1501-1514.
[13] R. Doherty, A. Mullane, G. Nolan, D.J. Burke, A. Bryson, M. O'Malley, An assessment of the impact of wind generation on system frequency control, Power Systems, IEEE Transactions on, 25 (2010) 452-460.
[14] R. Yan, T.K. Saha, N. Modi, N.-A. Masood, M. Mosadeghy, The combined effects of high penetration of wind and PV on power system frequency response, Applied Energy, 145 (2015) 320-330.
[15] A. Keyhani, A. Chatterjee, Automatic generation control structure for smart power grids, Smart Grid, IEEE Transactions on, 3 (2012) 1310-1316.
[16] H. Golpîra, M.R. Haghifam, H. Seifi, Dynamic power system equivalence considering distributed energy resources using Prony analysis, International Transactions on Electrical Energy Systems, 25 (2015) 1539-1551.
[17] M. Lemmon, Advanced Distribution and Control for Hybrid Intelligent Power Systems, in, Dept. of Electrical Engineering, University of Notre Dame, 2011.
[18] H. Golpîra, M.R. Haghifam, H. Seifi, Dynamic Equivalencing of an Active Distribution Network for Large-Scale Power System Frequency Stability Studies, IET Generation, Transmission & Distribution, 9 (2015) 2245-2254.
[19] H. Bevrani, J. Raisch, On Virtual Inertia Application in Power Grid frequency Control, Energy Procedia, 141 (2017) 681-688.
[20] U.O. Handbook, P1–Policy 1: Load-Frequency Control and Performance [C], Version: v3. 0 rev, 15 (2009).
[21] Nerc, Standard BAL-003-1 — Frequency Response and Frequency Bias Setting, (2013).
[22] H. Bevrani, T. Hiyama, Intelligent automatic generation control, CRC press, 2017.
[23] J. Chow, G. Rogers, Power system toolbox, Cherry Tree Scientific Software,[Online] Available: http://www.ecse.rpi.edu/pst/PST.html, (2000).